

Research Article

Failure Analysis of Rolling Contact Bearing for Flywheel Energy Storage Systems

Lijesh K.P.^{†*}, S.M. Muzakkir[†] and Harish Hirani[†]

[†]Mechanical Engineering Department, Indian Institute of Technology, Delhi, New Delhi, India

Accepted 15 Feb 2015, Available online 21 Feb 2015, Vol.5, No.1 (Feb 2015)

Abstract

In recent past, lead acid batteries have been replaced by flywheels in the energy storage systems (ESS). The performance of a flywheel energy storage system (FESS) greatly depends on the performance of the supporting bearings. To study the performance of FESS incorporating ball bearings, a test setup was developed consisting of one 20 kg flywheel and two ball bearings. The performance of FESS was evaluated by measuring the time to coasting down of flywheel. With the number of operation of FESS, performance deterioration was observed. The condition monitoring unit, consisting of accelerometer and eddy current proximity sensor, was installed to investigate reason(s) of reduction in the performance. On analyzing acceleration and FFT plots, the failure of bearing(s) was diagnosed. To confirm the failure prediction, the bearing was dismantled and visual inspection was carried out.

Keywords: FESS, Ball bearing, condition monitoring, FFT

1. Introduction

In the most commonly of ESS, lead acid batteries are used as power backup. There is growing trend to replace lead acid batteries as those batteries are environmental hazardous and provide slow response, limited life, and drop in voltage during discharge. In other words, there is a need to replace the existing batteries with a maintenance free and green product. One such technology is flywheel energy storage system (FESS), which consists of a flywheel to store energy in form of kinetic energy. To store more kinetic energy, the higher value of angular velocity ' ω ' is preferred. But increase in velocity increases the dynamic load (due to unbalance mass), so appropriate selection/design of bearings is mandatory. The minimum power loss during acceleration (charging)/ deceleration (discharging) and the minimum response time to reach the rated speed are the main factors affecting the bearing selection/design.

Bearings can be broadly classified into three different categories (i) Magnetic bearings (MB) (Bornemann *et al*, 1994), (Lijesh and Hirani, 2015), (Lijesh and Hirani, 2015), (Lijesh and Hirani, 2014) (ii) Fluid Film bearing (Hirani, 2005), (Muzakir *et al*, 2011), (Muzakir *et al*, 2011) and (iii) Rolling bearings (Hirani, 2009), (Genta, 1985). The coefficient of friction can be restricted in the range of 0.000009 to 0.00005 (Hirani and Verma, 2009), (Hirani and Suh, 2005)

using the magnetic bearing compared to 0.001-0.002 for rolling bearing and 0.001-0.25 for journal bearing.

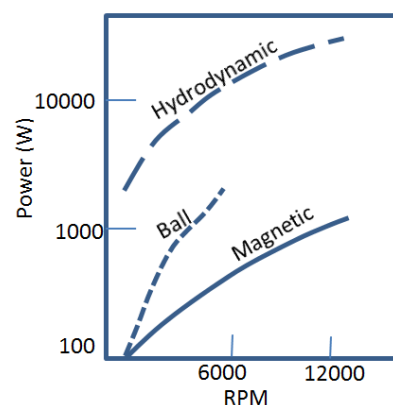


Fig. 1 Power dissipated by different types of bearing at different rotational speed (Genta, 1985)

The power dissipation for different bearing at various rotational speeds is plotted in the figure 1 (Genta, 1985). The plot is obtained for 1000 kg mass rotor. From the plot it can be noted that magnetic bearing dissipates less power compared to the rolling and hydrodynamic bearings. The magnetic bearings are strongly recommended for FESS due to its non-contact operation. Magnetic bearing are of two types (i) Passive magnetic bearing (Lijesh and Hirani, 2014), (Muzakir *et al*, 2014), (Lijesh and Hirani, 2015) and (ii) Active magnetic bearing (Shankar *et al*, 2006), (Chittlangia *et al*, 2014). The Passive Magnetic Bearing

*Corresponding author: Lijesh K.P.

(PMB) has low load carrying capacity (Hirani, and Samanta, 2007) (Samanta and Hirani, 2007) and as per Earnshaw theory (Earnshaw, 1839), the bearing is unstable in one of its axis which requires secondary arrangement to provide stability. Active Magnetic Bearing (AMB) incurs high initial and running costs and also requires complex control algorithm to control the shaft position. These reasons discourage to use magnetic bearing for FESS. Due to high consumption of power (Genta, 1985) and continuous supply of liquid lubricant, the hydrodynamic bearings should not be used for flywheel applications. Ball bearings provide economic solution for FESS.

The ball bearing is selected considering type and magnitude of load, speed, life, and requirements of seals. The bearing life is dependent upon the loading cycles and magnitude of load. The efficiency of a FESS is estimated by determining the coasting down time i.e. time taken by the flywheel to come to rest from a rotating speed. In the present research work, an experimental set up was developed to study the performance of FESS with ball bearings. It was observed that the performance of the flywheel was reducing with number of experiments performed on it. To understand the reason for the failure of the bearing, the signals acquired from accelerometer and proximity sensors were analyzed and the predicted reason for failure from theory was been confirmed by dismantling the ball bearing.

2. Experimental Results and Discussion

Figure 2 shows the experimental setup considered for the present work. This test setup consist of a 5hp motor with controller, flywheel of 20kg, two ball bearings; (i) bearing 1: bearing no.6210 and (ii) bearing 2: bearing no.6209. The accelerometer and proximity sensors were used to measure the acceleration and key phasor signals. The signals were stored in computer using LABVIEW software. The acceleration signals provide information on the vibration and natural frequency of the system; while the displacement signals provide information of the motor speed. Accelerometer was mounted on one of the bearings (i.e. bearing 1) and proximity sensor was mounted below the coupling screw to acquire the key-phasor signal.

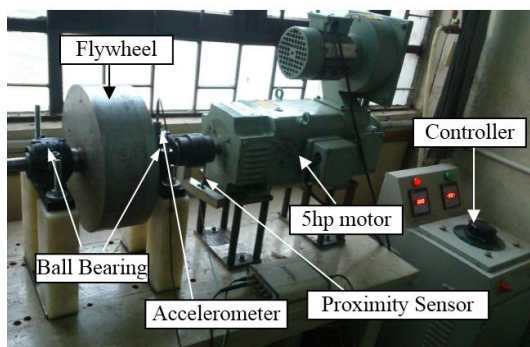
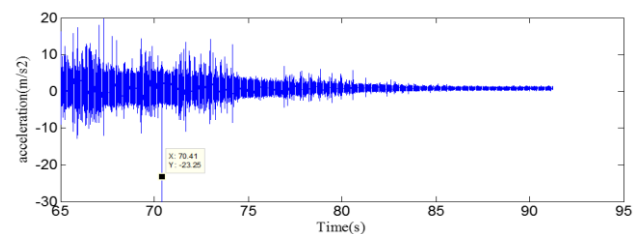
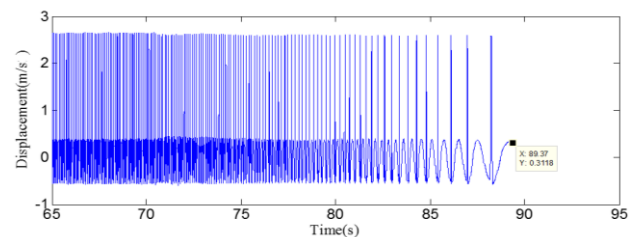


Fig. 2 FESS experimental setup

The motor was rotated at 420 RPM and the motor was switched off to analyze the performance during the coasting down of flywheel. Experiments at constant motor speed using Fast Fourier Transform (FFT) provide an estimation of system natural frequencies; while coasting down experiments by switching off the motor and recording the time for flywheel to reach zero rpm from certain rotational rpm provide the performance of FESS.



(a) Acceleration Signal



(b) Displacement signal

Fig. 3 Acceleration and displacement signals during coasting down

The acquired acceleration and displacement signals during the coasting down time of the flywheel are plotted in figure 3(a) and 3(b). From these figures, it can be observed that during the coasting down of the flywheel, disturbing signal was observed and which would have resulted in reducing the flywheel rotation time. When the motor was switched off there was a spike in acceleration signal which denotes the starting of coasting down and time for the flywheel to come to rest was observed from the displacement signals as depicted in figure 3. The estimating time for coasting down for the flywheel was 18.96sec.

To predict the reason for disturbing signals, accelerometer signal measured at 420 RPM shown in figures 4(a) was analyzed for estimating natural frequencies of the system using FFT. In acceleration signals steep increase of signal was observed which indicates the failure of the one of the components of ball bearing (balls, inner or outer race). To predict the exact reason of failure, FFT signals were plotted from the obtained acceleration signals (as shown in figures 4 (b) and 4(c)). Figure 4(b) shows the full FFT plot for 0-10,000Hz while figure 4(c) shows the zoomed plot of figure 4(b) i.e. FFT plot for 0- 200Hz. For ball bearing having pitch diameter (D), ball diameter (d), contact angle (ϕ) and 'n' number of balls, ball spin frequency (BSF), Ball Pass Frequency Outer race (BPFO) and Ball

Pass Frequency Inner races (BPFI) are estimated using equations (1-3) respectively.

$$BSF = \frac{D}{2d} \left(1 - \left(\frac{d}{D} \cos \phi \right)^2 \right) \tag{1}$$

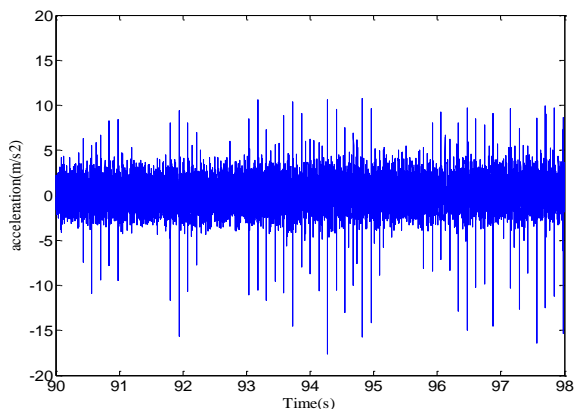
$$BPFO = \frac{nf_r}{2} \left(1 - \frac{d}{D} \cos \phi \right) \tag{2}$$

$$BPFI = \frac{nf_r}{2} \left(1 + \frac{d}{D} \cos \phi \right) \tag{3}$$

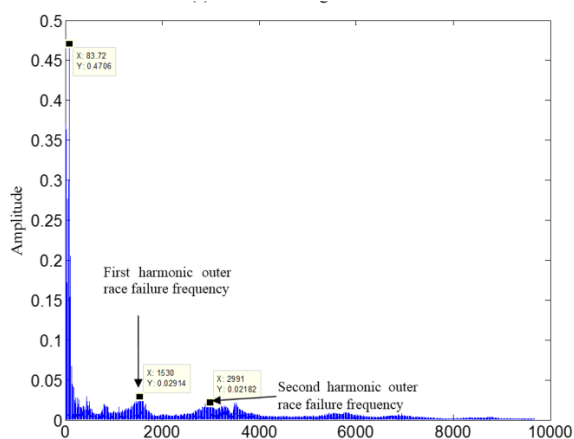
Dimension of the bearings, used in the present setup, and corresponding failure frequencies are listed in table 1.

Table 1 Dimensions and estimated failure frequency

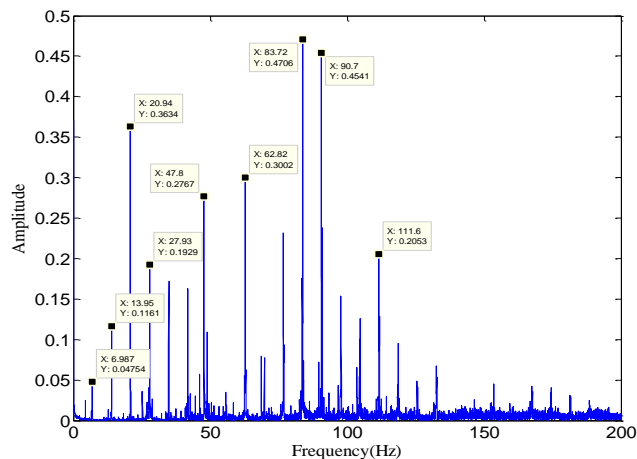
Ball Bearing no.	6209	6210
D (mm)	85	90
d (mm)	45	50
n	9	10
fr	420	420
BSF	1033	1117
BPFO	1520	1718
BPFI	2872	3267



(a) Acceleration signal



(b) FFT plot

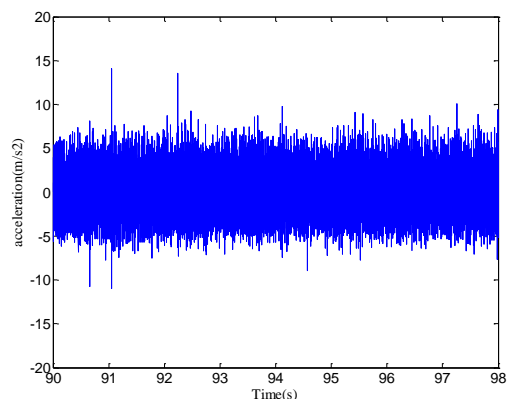


(c) Zoomed vies of FFT plot

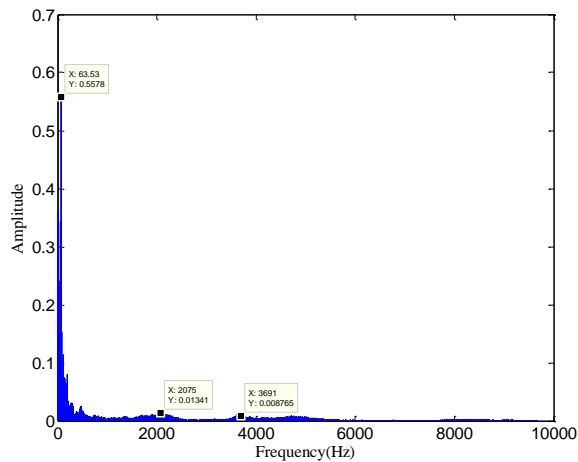
Fig. 4 acceleration and FFT plot for bearing 1

Comparing the peak value of frequencies illustrated in figure 5(b) and theoretically estimated frequencies from table 1, it can be concluded that the outer race of the bearing 1 has failed. The magnitudes of FFT plot indicates that the failure of the outer race is at the starting stage. Peaks in figure 4(c) indicates the motor running frequency (420/60=7Hz) and its harmonics (side bands). The side bands signify the misalignment in the flywheel setup and may be the reason for the failure of the bearing.

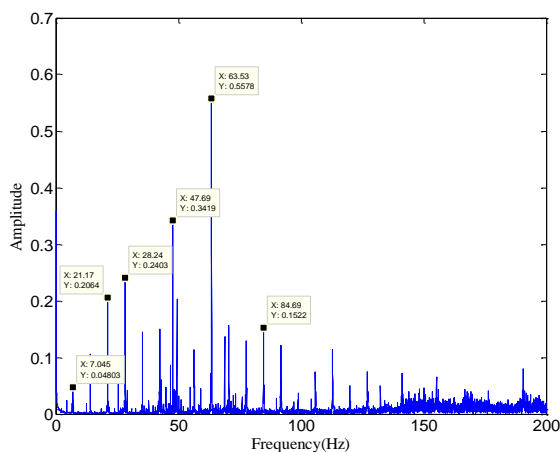
The Above procedure was followed for the second bearing bearing2, the acceleration signal and the FFT plot are shown in figures 5(a) and 5(b) respectively. From figure 5(a) it can be observed that the acceleration is constant throughout and there is no disturbing signal. From figure 4(b) ball bearing failure frequency was not observed. The zoomed view of figure 5(b) is plotted in figure 5(c) which indicates the harmonics of the motor frequency which again indicates the occurrence of misalignment in the system.



(a) Acceleration signal



(b) FFT plot



(c) Zoomed view of FFT

Fig.5 Acceleration and FFT plot for bearing 2

From the above discussions, it can be concluded that the bearing 1 is at the starting stage of the failure and the reason for the failure is misalignment while bearing 2 is performing its function. To confirm these conclusions, the bearing 1 was dismantled. The dismantled bearing is shown in figure 6. From figures 6(a) and 6(b), scars on the outer race and balls can be observed. The misalignment in the bearing and casing has led to the failure of the bearing and failure of flywheel system.

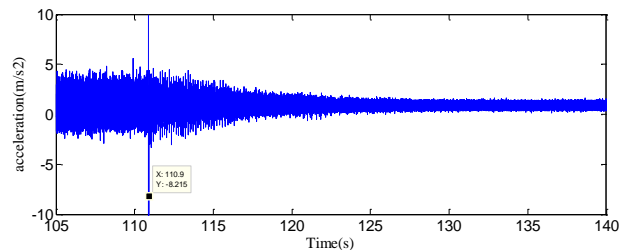


(a) Balls

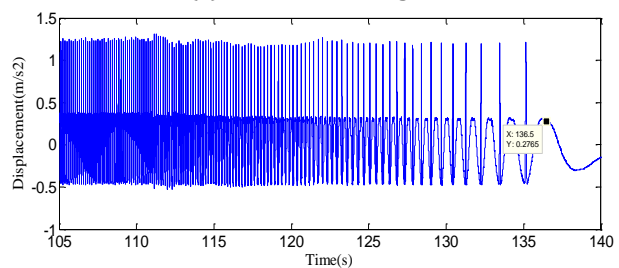
(b) Outer Race

Fig. 6 Scratches in ball and outer race

The misalignment in the bearing was rectified. The experiments were performed and the acceleration and displacement signals during the coasting down of flywheel were recorded. The signals are plotted in figure 7(a) and 7(b) respectively. In figure 7(a), no disturbing signal was observed and from displacement signal the time for coasting down was observed to be 26.3sec which is 7.34sec more than the failure system.



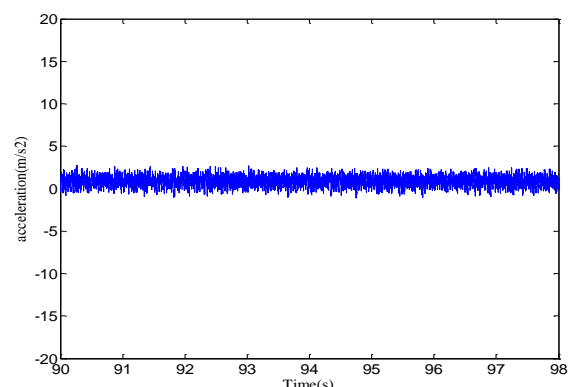
(a) Acceleration Signal



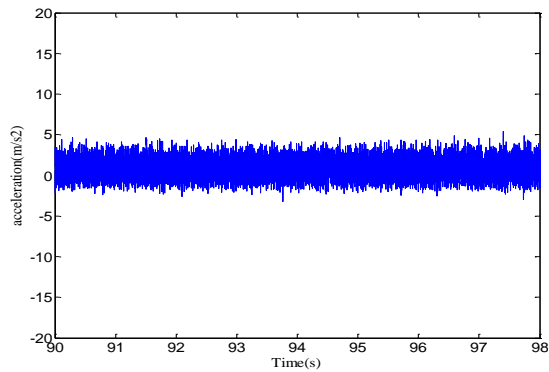
(b) Displacement signal

Fig. 7 Acceleration and displacement signals during coasting down for good bearing

Figures 8(a) and 8(b) shows the acceleration plot for bearing 1 and bearing 2 respectively. From these plots it can be observed that the magnitudes of acceleration signals are not disturbing signals are reduced to great extent compared to the failed system. FFT plot for bearing 1 and bearing 2 are shown in figures 9(a) and 9(b) respectively. From FFT plots, no ball bearing failure frequency is observed. From these plots it can be inferred that the using the accelerometer signals alignment of a system can be analyzed before performing any experiments on FESS.

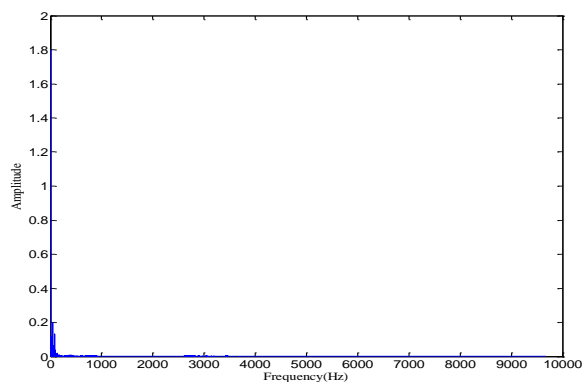


(a) Bearing 1

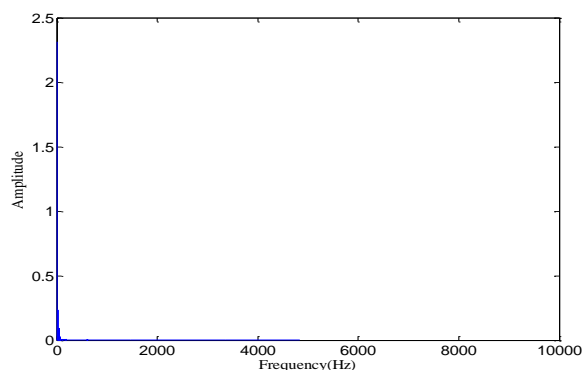


(b) Bearing 2

Fig. 8 Acceleration signal for bearing 1 and bearing 2



(a) Bearing 1



(b) Bearing 2

Fig. 9 FFT signal for bearing 1 and bearing 2

Conclusions

The deterioration in the performance of the FESS incorporating ball bearings was analyzed using accelerometer and proximity sensors. Using the accelerometer signals and FFT plots following conclusions shall be made:

- Several peaks in bearing 1 acceleration signal were observed, indicating failure of ball bearing.
- The ball pass frequency outer race of Bearing 1 was observed in the FFT signal indicating failure of outer ball race.

- Side bands in the FFT plot indicate the misalignment in the bearing which might be the reason for the failure of bearing.
- To confirm the prediction, ball bearing was dismantled and scratches in outer race and balls were observed indicating the prediction was correct. New bearing was installed by correcting the misalignment, the FFT and accelerometer plots indicated satisfactory performances.

References

- H.J. Bornemann, T. Ritter, C. Urban, O. paitsev, K. peber, and H. Rietschel,(1994), Low friction in a flywheel system pith passive superconducting magnetic bearings, Applied Superconductivity, 2(7-8), pp.439-447.
- K. P. Lijesh and H. Hirani, (2015), Optimization of Eight Pole Radial Active Magnetic Bearing, ASME, Journal of Tribology, 137(2), (7 pages).
- K.P. Lijesh and H. Hirani,(2015), Development of Analytical Equations for Design and Optimization of Axially Polarized Radial Passive Magnetic Bearing, ASME, Journal of Tribology, 137(1), (9 pages).
- K. P. Lijesh and H. Hirani,(2014), Design of eight pole radial active magnetic bearing using monotonicity, 9th International Conference on Industrial and Information Systems (ICIIS), IEEE, pp.1-6.
- H. Hirani,(2005), Multiobjective optimization of journal bearing using mass conserving and genetic algorithms, Proc. Institute Mech. Engineers., Part J, Journal of Engineering Tribology, 219(3), pp. 235-248.
- S. M. Muzakkir, H. Hirani, G. D. Thakre and M. R. Tyagi, (2011), Tribological Failure Analysis of Journal Bearings used in Sugar Mill, Engineering Failure Analysis, Volume 18, Issue 8, pp. 2093-2103.
- M. M. Khonsari and E. R. Booser, (2001), Applied tribology: Bearing design and Lubrication, Jhon Wiley and Sons. Inc., pp-11-12.
- H. Hirani, (2009), Root cause failure analysis of outer ring fracture of four row cylindrical roller bearing, Tribology Transactions, 52(2), pp.180-190.
- G. Genta, (1985), Kinetic Energy Storage: Theory and Practice of Advanced Flywheel Systems, Butterworth-Heinemann Ltd, London, pp. 214-215.
- H. Hirani and M. Verma, (2009), Tribological study of elastomeric bearings of marine shaft system, Tribology International, 42(2), 378-390.
- H. Hirani and N. P. Suh,(2005), Journal Bearing Design using Multiobjective Genetic Algorithm and Axiomatic Design Approaches, Tribology International, 38 (5), pp.481-491.
- K. P. Lijesh and H. Hirani, (2014), Stiffness and Damping Coefficients for Rubber mounted Hybrid Bearing, Lubrication Science, 26(5), pp. 301-314.
- S.M. Muzzakir, K.P. Lijesh and H. Hirani,(2014), Tribological Failure Analysis of a Heavily-Loaded Slow Speed Hybrid Journal Bearing, Engineering Failure Analysis, 40, 97-113.
- K. P. Lijesh and H. Hirani,(2015), The Performance of Hybrid Journal Bearing under Extreme Operating Conditions, International Journal of Current Engineering and Technology, 5(1),pp.277-282.
- S. Shankar, Sandeep and H. Hirani,(2006), Active Magnetic Bearing, Indian Journal of Tribology, pp 15-25.
- V. Chittlangia, K. P. Lijesh, A. Kumar, and H. Hirani,(2014), optimum Design of an Active Magneitic Bearing Considering the Geometric Programming, Technology Letters, 1(3), pp. 23-30.
- S. Earnshaw,(1839), On the nature of molecular forces which regulate the constitution of luminiferous ether, Trans. Cambridge Phil. Soc, 7, pp. 97-112.
- H. Hirani, and P. Samanta, (2007), Hybrid (Hydrodynamic + Permanent Magnetic) Journal Bearings, Proc. Institute Mech. Engineers., Part J, Journal of Engineering Tribology, 221(8), pp. 881-891.
- P Samanta and H Hirani, (2008), Magnetic Bearing Configurations: Theoretical and Experimental Studies, IEEE Transactions on Magnetics, 44 (2), pp. 292-300.
- K. P. Lijesh, H. Hirani, P. Samanta, Effect of Molybdenum Disulphide on Physical Properties of Neodymium-Iron-Boron Bonded Magnet, IJMER 2015, 5 (2), pp: 11-16.